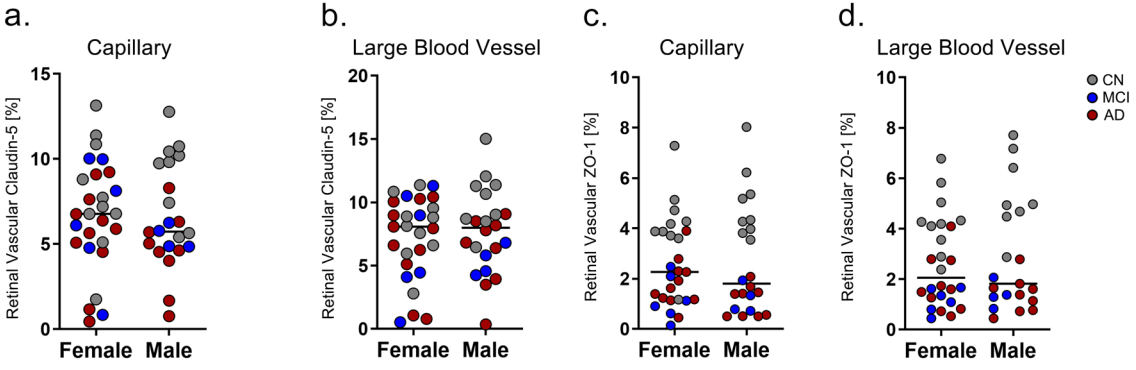

Supplementary figure 1. Sex-related differences in expression of claudin-5 and ZO-1 in retinal blood vessels. **a-b**. Quantitative analyses of retinal vascular claudin-5 immunoreactivity (IR) in **a**. capillaries and **b**. large blood vessels stratified by sex in the cohort specified in figure 1a (n=53 total). **c-d**. Quantitative analyses of retinal vascular ZO-1 IR in **c**. capillaries and **d**. large blood vessels stratified by sex in the cohort specified in figures 2e-f (n=53 total). Data from individual donors (circles) as well as group means ± SEMs are shown.

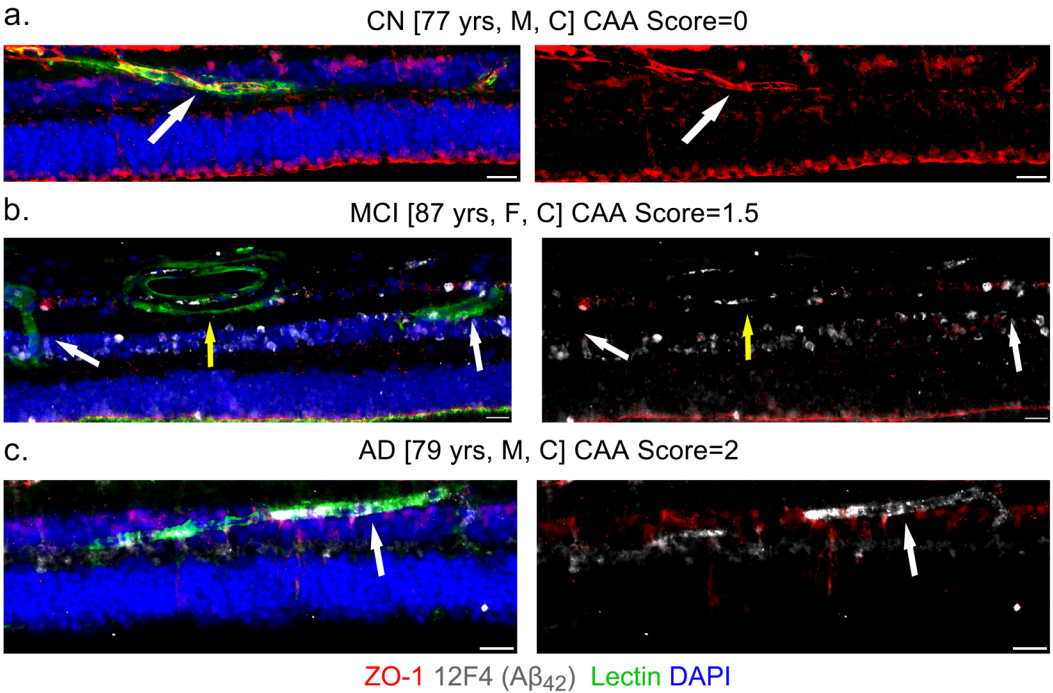

Supplementary figure 2. Additional representative images showing ZO-1 expression in retinal blood vessels. **a-c.** Representative images of immunofluorescent staining for ZO-1 (red), 12F4 ($A\beta_{42}$, white), lectin (green), and DAPI (blue) on postmortem retinal cross-sections from MCI (n=10) and AD (n=21) patients versus CN controls (n=22). yrs=years old; M=male; F=female; C=Caucasian; all scale bars=20μm. White arrows indicate capillaries. Yellow arrows indicate arterioles.

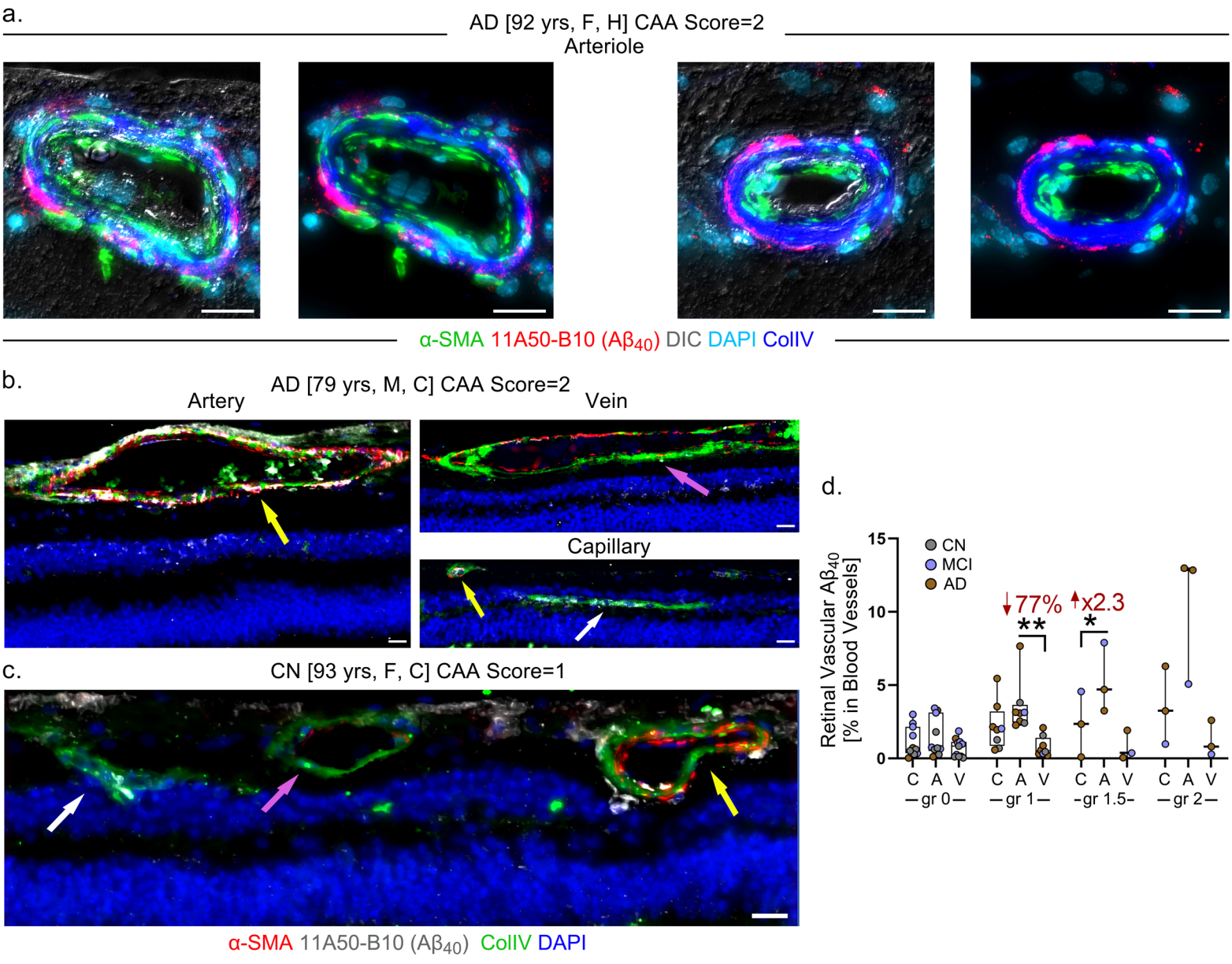

Supplementary figure 3. Additional representative images and data analyses for retinal vascular Aβ$_{40}$. **a**. Representative images showing immunofluorescent staining of arteriolar 11A50-B10 (Aβ$_{40}$, red), α-SMA (green), collagen IV (ColIV, blue), and DAPI (cyan) with differential interference contrast (DIC) channel on postmortem retinal cross-sections from MCI (n=8) and AD (n=15) patients versus CN controls (n=15). **b-c**. Representative images showing immunofluorescent staining of 11A50-B10 (Aβ$_{40}$, white) in arteries and capillaries versus veins, α-SMA (red), collagen IV (ColIV, green), and DAPI (blue) on postmortem retinal cross-sections from the same cohort (n=38 total). **d**. Quantitative analysis of retinal vascular Aβ$_{40}$ immunoreactivity stratified by blood vessel type and CAA severity score in the same cohort (n=38 total). yrs=years old; F=female; M=male; H=Hispanic; C=-Caucasian. White arrows indicate capillaries. Yellow arrows indicate arterioles. Magenta arrows indicate venules. All scale bars=20μm. Data from individual donors (circles) as well as group means ± SEMs are shown. *p < 0.05, **p < 0.01, by two-way ANOVA with Tukey's post-hoc multiple comparison test. Fold changes and percentage decreases are shown in red.

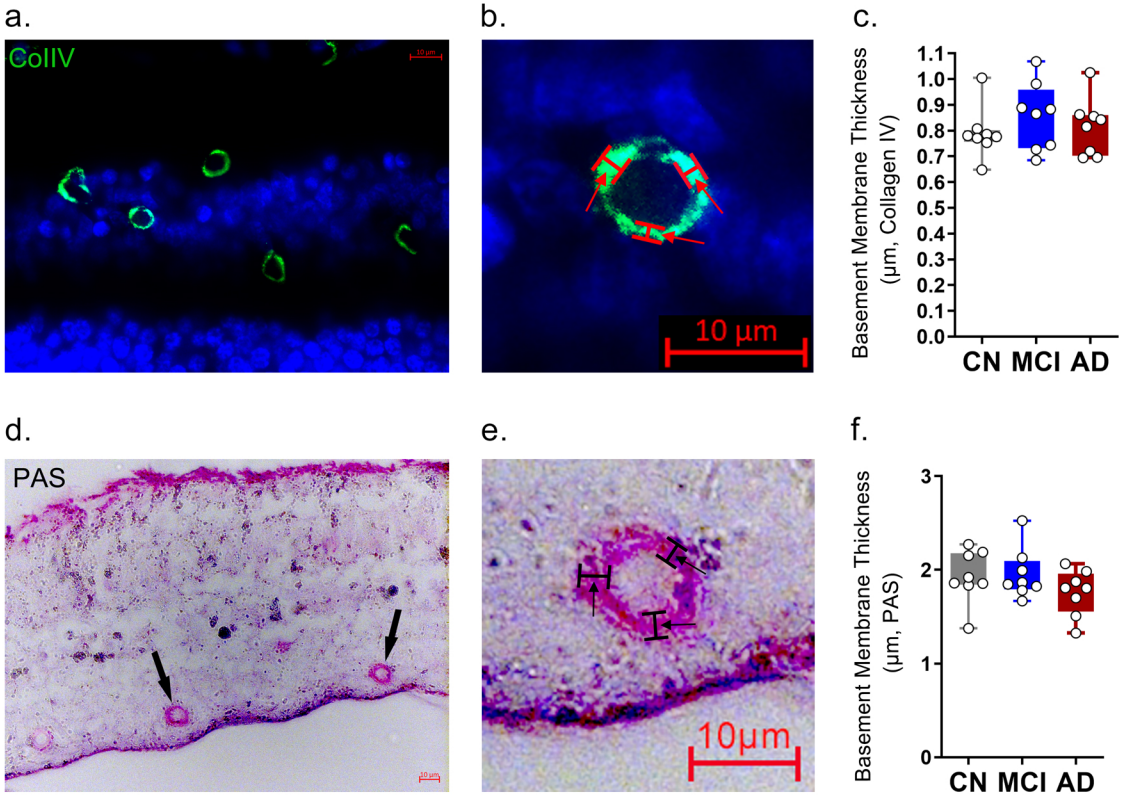

Supplementary figure 4. Measurements of basement membrane (BM) thickness in retinal capillaries. **a**. Representative images for immunofluorescent staining of collagen IV (ColIV) showing retinal capillaries (diameter≤10µm). **b**. An example showing measurements of BM thickness based on ColIV staining in ZEN 2.6 blue edition software. 3 measurements of each blood vessel were performed. **c**. Quantitative analysis of capillary BM thickness based on measuring collagen IV staining (n=24 total). **d**. Representative images for periodic acid/Schiff (PAS) staining showing retinal capillaries (diameter≤10µm). **e.** An example showing measurements of BM thickness based on PAS staining in ZEN 2.6 blue edition software. 3 measurements of each blood vessel were performed. **f.** Quantitative analysis of capillary BM thickness based on measuring PAS staining (n=24 total). All scale bars=10µm. Data from individual donor (circles) as well as group means ± SEMs are shown. One-way ANOVA with Tukey's post-hoc multiple comparison test were performed.

Supplementary Table 1. Information on human donors included in the study

Donor	Sex	Race	Age at death	Thal-A	Braak-B	CERAD-C	CAA Score	Co-morbid. [LB/ASVD]	Braak Stage	CDR Score	MMSE Score	APOE status	Study type
AD1	F	C	93	2	3	3	1	−/+	V	3	n.a.	n.a.	IHC /MS
AD2	M	H	97	3	2	3	1	−/+	III	n.a.	n.a.	n.a.	IHC
AD3	M	C	79	3	3	3	1.5	−/+	V	n.a.	n.a.	n.a.	IHC
AD4	F	C	87	3	3	3	n.a.	−/+	V-VI	n.a.	n.a.	n.a.	IHC
AD5	M	C	88	2	3	2	1	−/+	V-VI	1	18	e3/e4	IHC /MS
AD6	M	C	77	3	3	3	1	−/−	VI	2	n.a.	e3/e4	IHC
AD7	F	C	66	3	3	3	0	−/+	VI	3	n.a.	e3/e3	IHC
AD8	F	H	99	3	2	3	1.5	−/−	IV	n.a.	n.a.	n.a.	IHC
AD9	F	H	81	3	3	3	1.5	−/+	V-VI	3	n.a.	e3/e3	IHC
AD10	F	C	90	3	3	3	1	−/+	V-VI	3	n.a.	e3/e4	IHC
AD11	M	C	90	3	2	3	1	−/+	III-IV	3	1	e3/e4	IHC
AD12	M	C	90	3	3	3	1	−/+	VI	3	n.a.	n.a.	IHC
AD13	F	C	90	1	3	3	1	−/+	V	2	9	n.a.	IHC
AD14	M	C	79	2	2	2	2	−/+	V	0.5	24	n.a.	IHC
AD15	F	H	92	2	2	2	2	−/+	III	3	n.a.	e3/e3	IHC
AD16	M	C	88	3	3	3	1.5	−/+	V-VI	1	16	e2/e3	IHC
AD17	F	B	94	3	3	3	0	−/+	V-VI	3	n.a.	e3/e3	IHC /MS
AD18	F	n.a.	87	n.a.	n.a.	n.a.	n.a.	n.a./n.a.	n.a.	n.a.	n.a.	n.a.	IHC
AD19	F	n.a.	70	n.a.	n.a.	n.a.	n.a.	n.a./n.a.	n.a.	n.a.	n.a.	n.a.	IHC
AD20	M	A	81	3	3	3	1	−/−	V	1	n.a.	e4/e4	IHC
AD21	M	C	79	3	1	3	n.a.	+/+	I	n.a.	n.a.	n.a.	IHC
MCI1	M	C	97	2	3	3	1	−/+	V	0.5	n.a.	e3/e3	IHC
MCI2	M	H	80	3	3	2	n.a.	−/+	V-VI	3	n.a.	e3/e3	IHC
MCI3	F	B	94	3	1	1	0	n.a./−	I-II	0.5	23	e3/e3	IHC
MCI4	F	C	89	1	2	2	1	−/+	III-IV	0.5	21	e3/e3	IHC
MCI5	F	C	93	3	2	2	2	−/+	IV	3	n.a.	e3/e3	IHC
MCI6	M	C	93	2	2	0	0	−/+	0	3	n.a.	e2/e3	IHC
MCI7	F	C	86	3	1	3	0	−/+	I-II	0	26	e3/e4	IHC
MCI8	M	C	88	1	2	2	0	−/+	III	0	24	n.a.	IHC
MCI9	F	C	80	n.a.	n.a.	n.a.	0	+/n.a.	IV	n.a.	n.a.	n.a.	IHC
MCI10	F	C	87	3	3	3	1.5	−/+	V-VI	3	n.a.	e3/e3	IHC
CN1	F	C	93	n.a.	n.a.	n.a.	n.a.	n.a.	n.a.	n.a.	n.a.	n.a.	IHC
CN2	F	C	86	n.a.	n.a.	n.a.	n.a.	n.a.	n.a.	n.a.	n.a.	n.a.	IHC
CN3	M	C	78	n.a.	n.a.	n.a.	n.a.	n.a.	n.a.	n.a.	n.a.	n.a.	IHC
CN4	M	H	76	n.a.	n.a.	n.a.	n.a.	n.a.	n.a.	n.a.	n.a.	n.a.	IHC
CN5	M	C	95	1	1	1	0	−/−	I	0	n.a.	e3/e3	IHC

CN6	F	C	88	n.a.	n.a.	n.a.	n.a.	n.a.	n.a.	n.a.	n.a.	n.a.	IHC
CN7	M	H	81	3	2	2	0	−/+	I-II	0	23	e3/e4	IHC /MS
CN8	F	C	99	1	2	1	0	−/−	III	0	n.a.	e3/e3	IHC
CN9	F	C	92	n.a.	n.a.	n.a.	0	−/+	I-II	n.a.	25	n.a.	IHC
CN10	M	C	69	n.a.	n.a.	n.a.	0	−/+	0	n.a.	28	n.a.	IHC
CN11	F	C	91	n.a.	n.a.	n.a.	0	−/+	III	n.a.	29	n.a.	IHC
CN12	M	C	77	n.a.	n.a.	n.a.	n.a.	n.a.	n.a.	n.a.	n.a.	n.a.	IHC
CN13	M	C	73	n.a.	n.a.	n.a.	n.a.	n.a.	n.a.	n.a.	n.a.	n.a.	IHC
CN14	M	C	84	n.a.	n.a.	n.a.	n.a.	n.a.	n.a.	n.a.	n.a.	n.a.	IHC
CN15	M	C	70	n.a.	n.a.	n.a.	n.a.	n.a.	n.a.	n.a.	n.a.	n.a.	IHC
CN16	F	C	95	3	3	2	1	−/+	V	0	30	e3/e3	IHC
CN17	F	C	93	3	2	3	1	−/+	III-IV	1	n.a.	e2/e3	IHC
CN18	F	H	85	2	1	2	0	−/+	I-II	0	30	e3/e3	IHC
CN19	M	B	80	n.a.	n.a.	n.a.	n.a.	n.a.	n.a.	n.a.	n.a.	n.a.	IHC
CN20	F	C	80	n.a.	n.a.	n.a.	n.a.	n.a.	n.a.	n.a.	n.a.	n.a.	IHC
CN21	M	C	58	n.a.	n.a.	n.a.	n.a.	n.a.	n.a.	n.a.	n.a.	n.a.	IHC
CN22	F	C	64	n.a.	n.a.	n.a.	n.a.	n.a.	n.a.	n.a.	n.a.	n.a.	IHC
AD22	F	H	48	n.a.	n.a.	n.a.	2	−/n.a.	V	n.a.	n.a.	n.a.	MS
AD23	M	W	72	n.a.	n.a.	n.a.	n.a.	n.a.	n.a.	n.a.	n.a.	n.a.	MS
AD24	F	W	100	2	3	3	0	−/+	V-VI	2	16	n.a.	MS
CN23	F	W	75	n.a.	n.a.	n.a.	n.a.	n.a.	n.a.	n.a.	n.a.	n.a.	MS
CN24	F	W	72	n.a.	n.a.	n.a.	n.a.	n.a.	n.a.	n.a.	n.a.	n.a.	MS
CN25	M	W	69	n.a.	n.a.	n.a.	n.a.	n.a.	n.a.	n.a.	n.a.	n.a.	MS
CN26	F	W	79	n.a.	n.a.	n.a.	n.a.	n.a.	n.a.	n.a.	n.a.	n.a.	MS
CN27	M	W	85	0	1	3	1	−/+	I-II	0.5	n.a.	n.a.	MS

Abbreviations: AD, Alzheimer's disease dementia; MCI, mild cognitive impairment; CN, cognitively normal; F, female; M, male; A, Asian; B, Black; H, Hispanic; W, White; IHC, Immunohistochemistry; MS, mass spectrometry; A, Aβ plaque score modified from Thal; B, NFT stage modified from Braak; C, Neuritic plaque score modified from CERAD; CAA, Cerebral amyloid angiopathy; LB, Lewy bodies; ASVD. Atherosclerosis; CDR, Clinical Dementia Rating; MMSE, Mini-Mental State Examination; n.a., not available; +, present; –, none; APOE, apolipoprotein alleles.

Supplementary Table 2. List of antibodies.

Antibodies or Reagents	Source Species	Dilution	Application	Commercial Source	Catalog. #
Primary antibody					
Claudin-5 mAb	Mouse	1:20	IF	Thermofisher	35-2500
Collagen IV pAb	Rabbit	1:500	IF	Abcam	ab6586
Alexa Fluor 488-conjugated tomato lectin	*Lycopersicon esculentum*	1:200	IF	Dylight	DL-1174
$A\beta_{42}$ (12F4) mAb	Mouse	1:200	IF	Biolegend	805501
$A\beta_{40}$ (11A50-B10) mAb	Mouse	1:200	IF	Biolegend	805401
Zonula Occluden-1 pAb	Rabbit	1:50	IF	Thermofisher	61-7300
α-smooth muscle actin pAb	Goat	1:250	IF	Thermofisher	51-9000
JRF/cA$\beta_{40/28}$ # 8152 mAb	Mouse	1:2000	IF	Janssen Pharmaceutical	JRF/cA$\beta_{40/28}$ # 8152 mAb
Secondary antibody					
Cy2 (anti-Rabbit)	Donkey	1:200	IF	Jackson ImmunoResearch Laboratories	
Cy3 (anti-rabbit, anti-goat, anti-mouse)	Donkey	1:200	IF	Jackson ImmunoResearch Laboratories	
Cy5 (anti-mouse)	Donkey	1:200	IF	Jackson ImmunoResearch Laboratories	

Abbreviation: IF – immunofluorescence; pAb – polyclonal antibody; mAb – monoclonal antibody.

Extended Methods

Postmortem eyes from human donors. Human eye tissues collected from donor patients with premortem clinical diagnoses of MCI and AD dementia (and confirmed postmortem AD neuropathology), and age- and sex-matched CN controls (total n=61 subjects) were primarily obtained from the Alzheimer's Disease Research Center (ADRC) Neuropathology Core in the Department of Pathology (IRB protocol HS-042071) of Keck School of Medicine at the University of Southern California (USC, Los Angeles, CA). Additional eyes were obtained from the National Disease Research Interchange (NDRI, Philadelphia, PA) under approved Cedars-Sinai Medical Center IRB protocol Pro00019393. USC-ADRC and NDRI maintain human tissue collection protocols that are approved by their managerial committees and subject to oversight by the National Institutes of Health. Histological studies at Cedars-Sinai Medical Center were performed under IRB protocols Pro00053412 and Pro00019393. For histological examinations, 53 retinas were collected from deceased donors with confirmed AD (n=21), MCI due to AD (n=10), as well as from age- and sex-matched deceased donors with CN (n=22). For mass spectrometry analyses, eyes were collected from another deceased donor cohort (n=12) comprised of clinically and neuropathologically confirmed AD patients (n=6) and matched NC controls (n=6). Demographic, clinical, and neuropathological information on human donors is detailed in **Table 1** and **Table 2**. Patients' identity was protected by de-identifying all tissue samples in a manner not allowing to be traced back to tissue donors.

Clinical and neuropathological assessments. ADRC provided the clinical and neuropathological reports on the patients' neurological examinations, neuropsychological and cognitive tests, family history, and medication lists as collected in the ADRC system using the Unified Data Set (UDS) [1]. The NDRI provided the medical history of additional patients. Most cognitive evaluations had been performed annually and, in most cases, less than one year prior to death. Cognitive testing scores from evaluations made closest to the patient's death were used for this analysis. Two global indicators of cognitive status were used for clinical assessment: the Clinical Dementia Rating (CDR scores: 0 = normal; 0.5 = very mild impairment; 1 = mild dementia; 2 = moderate dementia; or 3 = severe dementia) [2] and the Mini-Mental State Examination (MMSE scores: normal cognition = 24–30; MCI = 20–23; moderate dementia = 10–19; or severe dementia ≤ 9) [3]. In this study, the composition of the clinical diagnostic group (AD, MCI, or CN) was determined by source clinicians based on findings of a comprehensive battery of tests including neurological examinations, neuropsychological evaluations, and the aforementioned cognitive tests. To obtain a final diagnosis based on the neuropathological reports, we used the modified Consortium to Establish a Registry for Alzheimer's Disease (CERAD) [4,5], as outlined in the National Institute on Aging (NIA)/Regan protocols with revision by the NIA and Alzheimer's Association [6]. The Aβ burden (measured as diffuse, immature, or mature plaques), amyloid angiopathy, neuritic plaques, neurofibrillary tangles (NFTs), neuropil threads (NTs), granulovacuolar degeneration, Lewy bodies, Hirano bodies, Pick bodies, balloon cells, neuronal loss, microvascular changes, and gliosis pathology were assessed in multiple brain areas, specifically in the hippocampus, entorhinal cortex, basal ganglia, midbrain [substantia nigra], pons [locus ceruleus] medulla and frontal, temporal, parietal, and occipital lobes. All cases underwent uniform brain sampling by a neuropathologist.

Cerebral amyloid plaques, NFTs, and NTs were evaluated using anti–β-amyloid mAb clone 4G8 immunostaining, Thioflavin-S (ThioS) histochemical stain, and Gallyas silver stain in formalin-fixed, paraffin-embedded tissue sections. Neuropathologists (Chief, Dr. Carol Miller and Dr. Debra Hawes) provided severity scores based on semi-quantitative observations. The scale for Aβ/neuritic plaques was determined by 4G8- and/or Thioflavin-S-positive and/or Gallyas silver-positive plaques measured per 1 mm^2 brain area (0 = none; 1 = sparse [≤ 5 plaques]; 3 = moderate [6–20 plaques]; 5 = abundant/frequent [21–30 plaques or greater]; or N/A = not applicable), as previously described [7]; NACC NP Guidebook, Version 10, January 2014: https://naccdata.org/data-collection/forms-documentation/np-10]. Brain NFT or NT severity scoring system was derived from observed burden of these AD neuropathologic changes detected by Gallyas silver and/or Thioflavin-S staining [7-9] and measured per 1 mm^2 brain area. The assigned NFT or NT scores are as following: 0 = none; 1 = sparse (mild burden); 3 = moderate (intermediate burden);

or 5 = frequent (severe burden). In both histochemical and immunohistochemical staining, each anatomic area of interest is assessed for the relevant pathology using the 20X objective (200X high power magnification) and representative fields are graded using a semiquantitative scale as detailed above. Validation of AD neuropathic change (ADNP), especially NTs, is performed using the 40X objectives (400X high power magnification); an average of 2 readings was assigned to each individual patient.

A final diagnosis included AD neuropathological change using an "ABC" score derived from 3 separate 4-point scales. We used the modified Aβ plaque Thal score (A0 = no Aβ or amyloid plaques; A1 = Thal phase 1 or 2; A2 = Thal phase 3; or A3 = Thal phase 4 or 5) [10]. For the NFT stage, the modified Braak staging for silver-based histochemistry or p-tau IHC was used (B0 = no NFTs; B1 = Braak stage I or II; B2 = Braak stage III or IV; or B3 = Braak stage V or VI) [11]. For the neuritic plaques, we used the modified CERAD score (C0 = no neuritic plaques; C1 = CERAD score sparse; C2 = CERAD score moderate; or C3 = CERAD score frequent) [4]. Neuronal loss, gliosis, granulovacuolar degeneration, Hirano bodies, Lewy bodies, Pick bodies, and balloon cells were all evaluated (0 = absent or 1 = present) in multiple brain areas by staining tissues with hematoxylin and eosin (H&E). Brain atrophy was evaluated (0 = none; 1 = mild; 3 = moderate; 5 = severe; or 9 = not applicable).

Processing of eye tissues. Donor eyes were collected within an average of 8 hours after time of death and were 1) preserved in Optisol-GS media (Bausch & Lomb, 50006-OPT) and stored at 4°C for less than 24 hours; 2) fresh frozen (snap frozen; stored at -80°C); or 3) punctured once and fixed in 10% neutral buffered formalin (NBF) or 4% paraformaldehyde (PFA) and stored at 4°C. Regardless of the source of the human donor eye (USC-ADRC or NDRI), the same tissue collection and processing methods were applied.

Preparation of retinal strips. Eyes that were fixed in 10% NBF or 4% PFA were dissected to create eyecups. The complete neurosensory retinas were isolated, detached from the choroid and sclera, flat mounts were prepared, and vitreous humor thoroughly removed manually, as previously described[12]. Alternatively, fresh-frozen eyes and eyes preserved in Optisol-GS were dissected, with the anterior chambers removed to create eyecups. Vitreous humor liquid was allowed to flow out and the complete neurosensory retina was isolated. Next, the vitreous gel was further thoroughly removed. Fresh-frozen retina was isolated in cold PBS with 1× Protease Inhibitor cocktail set I (Calbiochem 539131). For all flat mount retinas, the 4 topographical quadrants were defined by identifying the macula, optic disc (OD), and blood vessels [13]. Flat mount strips (~2mm wide) were prepared from superior-temporal retina, spanning diagonally from the OD to the ora serrata. Fixed retinal strips were processed for cross-sectioning. Fresh retinal strips (~5mm wide) were prepared and stored at -80°C for protein analysis. In a subset of freshly isolated donor eyes, additional ~2mm-wide strips were dissected and fixed in 4% PFA for processing of retinal cross-sections. Each strip measured approximately 2-2.5cm from the optic disc to the ora serrata. This sample preparation technique allowed for extensive and consistent access to retinal quadrants, layers, and pathological subregions.

Paraffin-embedded retinal cross-sections. Flat mount-derived strips were initially paraffinized using the standard techniques. Next, strips were embedded in paraffin after flip-rotating 90° horizontally. The retinal strips were sectioned (7-10µm thick) and placed on microscope slides treated with 3-aminopropyltriethoxysilane (APES, Sigma A3648). Before immunohistochemistry, the sections were deparaffinized with 100% xylene twice (10 min each), rehydrated with decreasing concentrations of ethanol (100% to 70%), and washed with distilled water followed by PBS.

Immunohistochemistry. Following deparaffinization, retinal sections were incubated in blocking buffer (Dako #X0909), followed by primary antibody incubation (information provided in **Supplementary table 2**) overnight in 4°C. Retinal sections were then washed 3 times by PBS and incubated with secondary antibodies against each species (1:200, information provided in **Supplementary table 2**) for 1 hr at RT.

After rinsing with PBS for 3 times, sections were mounted with Prolong Gold antifade reagent with DAPI (Thermo Fisher #P36935).

Periodic acid-Schiff (PAS) staining. For PAS staining of retinal vascular basement membranes (BM), retinal cross-sections were first rehydrated in distilled water for 15 min. The rehydrated samples were then incubated with periodic acid (MilliporeSigma, #P7875) solution at a concentration of 35 mM at room temperature (RT) for 8 min, followed by a brief dipping in distilled water. Afterward, the tissues were stained with Schiff (Sigma-Aldrich, #3952016) for 15 min, followed by three separate extensive washes in running distilled water lasting 5 min each time. After staining, the slides were dehydrated in 70%, 85%, 90% and 100% ethanol, and finally xylene, 2 min for each reagent. Following this, the slides were mounted with Permount mounting medium (Fisher Scientific, #SP15-100).

Microscopy. Fluorescence, bright field, and differential interference contrast (DIC) images were acquired using a Carl Zeiss Axio Imager Z1 fluorescence microscope with ZEN 2.6 blue edition software (Carl Zeiss MicroImaging, Inc.) equipped with ApoTome, AxioCam MRm, and AxioCam HRc cameras. Multi-channel image acquisition was used to create images with multiple channels. Images were repeatedly captured at the same focal planes with the same exposure time. Images were captured at 20×, 40×, and 63× objectives for different purposes.

Stereological Quantification. The fluorescence of specific signals was captured using the same setting and exposure time for each image by the Axio Imager Z1 microscope (with motorized Z-drive) with an AxioCam MRm monochrome camera (version 3.0; at a resolution of 1388 × 1040 pixels, 6.45 µm × 6.45 µm pixel size, and a dynamic range of >1:2200, which delivers low-noise images due to a Peltier-cooled sensor). Images were captured at 20x or 40x objectives, at a respective resolution of 0.25 µm. About twenty images were obtained from each retina to cover all types of blood vessels. Acquired images were converted to gray scale and standardized to baseline using a histogram-based threshold in the Fiji ImageJ (NIH) software program (version 1.53c). For each biomarker, the total area of immunoreactivity was determined using the same threshold percentage from the baseline in ImageJ (with the same percentage threshold setting for all diagnostic groups). The images were then subjected to particle analysis to determine the immunoreactive (IR) area fraction (%). Each data point was calculated by averaging the values in each type of blood vessels.

Measurements of retinal capillary basement membrane thickness: Two separate analyses of retinal capillary BM thickness were conducted: one involving immunostaining for collagen IV and the other using PAS staining. Images were captured at 63x objective. We used the distance measuring function in ZEN 2.6 blue edition software to perform these analyses. 3-5 capillaries with a diameter ≤10µm were measured in this study. For each blood vessel, we obtained 3 measurements and calculated the mean value.

Proteome Analysis by Mass Spectrometry (MS):
Preparation of retinal samples from CN and AD individuals. Frozen retinas (from the ADRC Neuropathology Core in the Department of Pathology at the University of Southern California, Los Angeles, CA) were processed for MS. Frozen tissues were transferred into a Precellys homogenization tube (Bertin Technologies), homogenized in liquid nitrogen, and lysed in ice-cold T-PER extraction buffer (Thermo Scientific) containing protease and phosphatase inhibitors. Next, tissue lysates were cleared of any debris by ultracentrifugation at 100,000g for 60 min at 4°C. Retinal tissues were carefully extracted from donor eye tissues without the vitreous and retinal pigment epithelium, and retinal temporal hemisphere (superiortemporal, inferiortemporal) tissues were homogenized (100 mM TEA Bromide [Sigma, 241059], 1% SDC [Sigma, D6750], and 1 × protease inhibitor cocktail set I [Calbiochem 539131]) by sonication (Qsonica Sonicator with M-Tip probe, amplitude 4, 6 W, for 90 seconds; the sonication pulse was stopped every 15 sec to allow the cell suspension to cool down for 10 sec). Insoluble materials were removed by centrifugation at 15,000 g for 10 min at 4°C. Protein concentrations of brain and retinal lysates were

determined via the Bradford assay (Bio-Rad Laboratories). Extracted retinal proteins were reduced using 5-mM DTT alkylation with 10 mM iodoacetamide. Protein concentration was determined using a BCA assay kit (Pierce). Dual digestion was carried out on 150 µg protein, initially using Lys-C (Wako, Japan) at a 1:100 enzyme:protein ratio overnight at RT followed by trypsin (Promega) at a 1:100 enzyme:protein ratio overnight at 37°C.

TMT Labeling. To accommodate 14 retinal samples (7 AD and 7 CN) for each corresponding tissue, 8 separate TMT10plex experiments were performed. 50-µg peptides from each sample were labeled with 0.8 mg TMT reagent. Labeling was carried out at RT for one hour with continuous vortexing. To quench any remaining TMT reagent and reverse the tyrosine labelling, 8 µl of 5% hydroxylamine was added to each tube, followed by vortexing and incubation for 15 min at RT. Combined samples from each TMT experiment were subjected to HpH fractionation using an Agilent 1260 HPLC system equipped with a quaternary pump, a degasser, and a multi-wavelength detector (set at 210-, 214- and 280-nm wavelengths). Peptides were separated on a 55-min linear gradient from 3 to 30% acetonitrile in 5 mM ammonia solution (pH 10.5) at a flow rate of 0.3 ml/minute on an Agilent 300 Extend C18 column (3.5-µm particles, 2.1-mm inner diameter, 150-mm length). The 96 fractions were finally consolidated into 17 fractions. Each peptide fraction was dried by vacuum centrifugation, resuspended in 1% formic acid, and desalted again using SDB-RPS (3M Empore) stage tips.

Nanoflow Liquid Chromatography Electrospray Ionization Tandem Mass Spectrometry (nano LC-ESI-MS/MS). Cleaned peptides from each fraction were analyzed using a Q Exactive Orbitrap mass spectrometer (Thermo Scientific) coupled to an EASY-nLC1000 nanoflow HPLC system (Thermo Scientific). Reversed-phase chromatographic separation was performed on an in-house packed reverse-phase column (75 µm × 10 cm Halo 2.7-µm 160 Å ES-C18, Advanced Materials Technology). Labeled peptides were separated for two hours using a gradient of 1%–30% solvent B (99.9% acetonitrile/0.1% formic acid) and Solvent A (97.9% water/2% acetonitrile/0.1% formic acid). The Q Exactive mass spectrometer (MS) was operated in the data-dependent acquisition mode to automatically switch between full MS and MS/MS acquisition. Following the full MS scan from m/z 350–1850, MS/MS spectra were acquired at a resolution of 70,000 at m/z 400 and an automatic gain control target value of 106 ions. The top 10 most abundant ions were selected with a precursor isolation width of 0.7 m/z for higher-energy collisional dissociation (HCD) fragmentation. HCD-normalized collision energy was set to 35%, and fragmentation ions were detected in the Orbitrap at a resolution of 70,000. Target ions that had been selected for MS/MS were dynamically excluded for 90 sec.

Database Searching, Peptide Quantification, and Statistical Analysis. Raw data files were processed with Proteome Discoverer V2.1 software (Thermo Scientific) using Mascot (Matrix Science, UK). Data were matched against the reviewed SwissProt *Homo sapiens* protein database. The MS1 tolerance was set to ± 10 ppm and the MS/MS tolerance to 0.02 Da. Carbamidomethyl (C) was set as a static modification, while TMT10-plex (N-term, K), oxidation (M), deamidation (N, Q), Glu->pyro-Glu (N-term E), Gln->pyro-Glu (N-term Q), and acetylation (Protein N-Terminus) were set as dynamic modifications. The percolator algorithm was used to discriminate correct from incorrect peptide-spectrum matches and to calculate statistics including q value (FDR) and posterior error probabilities. Search results were further filtered to retain protein with an FDR of <1%, and only master proteins assigned via the protein grouping algorithm were retained. Proteins were further analyzed using the TMTPrepPro analysis pipeline. TMTPrepPro scripts are implemented in the R programming language and are available as an R package, which was accessed through a graphic user interface provided by a local Gene Pattern server. In pairwise comparison tests, the relative quantitation of protein abundance was derived from the ratio of the TMT label S/N detected in each condition (AD *vs.* CN), and differentially expressed proteins (DEPs) were identified based on Student's t-tests between AD and CN group ratios (log-transformed). The overall fold changes were calculated as geometric means of the respective ratios. Differential expression required the proteins

to meet both a ratio fold change (>1.2 for upregulated or <0.80 for downregulated expression) and a p value cutoff (t-test $p < 0.05$).

Biological functions analysis (canonical pathway analyses) was performed using Ingenuity Pathway Analysis (IPA) by Qiagen.

Statistical Analysis. GraphPad Prism version 8.3.0 (GraphPad Software) was used for the analyses. Groups with two independent variables/factors were analyzed by using two-way ANOVA followed by Tukey's multiple comparison test to understand the interaction between the two independent variables. Three or more group comparisons were analyzed using one-way ANOVA followed by Tukey's multiple comparison test. Two-group comparisons were analyzed using a two-tailed unpaired Student t-test. The statistical association between two or more variables was determined using Pearson's correlation coefficient (r) test (Gaussian-distributed variables; GraphPad Prism). Pearson's r indicates the direction and strength of the linear relationship between two variables. Required sample sizes for two group (differential mean) comparisons were calculated using the nQUERY t-test model, assuming a two-sided α level of 0.05, 80% power, and unequal variances, with the means and common standard deviations for the different parameters. Results are expressed as means ± SEMs. A P value less than 0.05 is considered significant.

References:

1. Besser L, Kukull W, Knopman DS, et al. Version 3 of the National Alzheimer's Coordinating Center's Uniform Data Set. *Alzheimer Dis Assoc Disord*. Oct-Dec 2018;32(4):351-358. doi:10.1097/WAD.0000000000000279
2. Morris JC. The Clinical Dementia Rating (CDR): current version and scoring rules. *Neurology*. Nov 1993;43(11):2412-4. doi:10.1212/wnl.43.11.2412-a
3. Folstein MF, Folstein SE, McHugh PR. "Mini-mental state". A practical method for grading the cognitive state of patients for the clinician. *J Psychiatr Res*. Nov 1975;12(3):189-98. doi:10.1016/0022-3956(75)90026-6
4. Mirra SS, Heyman A, McKeel D, et al. The Consortium to Establish a Registry for Alzheimer's Disease (CERAD). Part II. Standardization of the neuropathologic assessment of Alzheimer's disease. *Neurology*. Apr 1991;41(4):479-86. doi:10.1212/wnl.41.4.479
5. Rossetti HC, Munro Cullum C, Hynan LS, Lacritz LH. The CERAD Neuropsychologic Battery Total Score and the progression of Alzheimer disease. *Alzheimer Dis Assoc Disord*. Apr-Jun 2010;24(2):138-42. doi:10.1097/WAD.0b013e3181b76415
6. Hyman BT, Phelps CH, Beach TG, et al. National Institute on Aging-Alzheimer's Association guidelines for the neuropathologic assessment of Alzheimer's disease. *Alzheimers Dement*. Jan 2012;8(1):1-13. doi:10.1016/j.jalz.2011.10.007
7. Montine TJ, Phelps CH, Beach TG, et al. National Institute on Aging-Alzheimer's Association guidelines for the neuropathologic assessment of Alzheimer's disease: a practical approach. *Acta Neuropathol*. Jan 2012;123(1):1-11. doi:10.1007/s00401-011-0910-3
8. Moloney CM, Lowe VJ, Murray ME. Visualization of neurofibrillary tangle maturity in Alzheimer's disease: A clinicopathologic perspective for biomarker research. *Alzheimers Dement*. Sep 2021;17(9):1554-1574. doi:10.1002/alz.12321
9. Uchihara T. Silver diagnosis in neuropathology: principles, practice and revised interpretation. *Acta Neuropathol*. May 2007;113(5):483-99. doi:10.1007/s00401-007-0200-2
10. Thal DR, Rub U, Orantes M, Braak H. Phases of A beta-deposition in the human brain and its relevance for the development of AD. *Neurology*. Jun 25 2002;58(12):1791-800. doi:10.1212/wnl.58.12.1791
11. Braak H, Alafuzoff I, Arzberger T, Kretzschmar H, Del Tredici K. Staging of Alzheimer disease-associated neurofibrillary pathology using paraffin sections and immunocytochemistry. *Acta Neuropathol*. Oct 2006;112(4):389-404. doi:10.1007/s00401-006-0127-z

12. Koronyo Y, Biggs D, Barron E, et al. Retinal amyloid pathology and proof-of-concept imaging trial in Alzheimer's disease. *JCI Insight*. Aug 17 2017;2(16)doi:10.1172/jci.insight.93621
13. Shi H, Koronyo Y, Rentsendorj A, et al. Identification of early pericyte loss and vascular amyloidosis in Alzheimer's disease retina. *Acta Neuropathol*. Feb 10 2020;doi:10.1007/s00401-020-02134-w